Talanta 122 (2014) 157–165

Contents lists available at ScienceDirect

Talanta

journal homepage: www.elsevier.com/locate/talanta

Fluorescence enhancement of CdTe MPA-capped quantum dots by glutathione for hydrogen peroxide determination

S. Sofia M. Rodrigues [a], David S.M. Ribeiro [a,*], L. Molina-Garcia [b], A. Ruiz Medina [b], João A.V. Prior [a], João L.M. Santos [a]

[a] Requimte, Department of Chemical Sciences, Laboratory of Applied Chemistry, Faculty of Pharmacy, University of Porto, Rua de Jorge Viterbo Ferreira no 228, 4050-313 Porto, Portugal

[b] Department of Physical and Analytical Chemistry, Faculty of Experimental Sciences, University of Jaén, Campus las Lagunillas, E-23071 Jaén, Spain

ARTICLE INFO

Article history:
Received 25 November 2013
Received in revised form
21 January 2014
Accepted 23 January 2014
Available online 31 January 2014

Keywords:
Fluorescence enhancing
Surface passivation
Glutathione
CdTe quantum dots
Flow analysis.

ABSTRACT

The manipulation of the surface chemistry of semiconductor nanocrystals has been exploited to implement distinct sensing strategies in many analytical applications. In this work, reduced glutathione (GSH) was added at reaction time, as an electron-donor ligand, to markedly increase the quantum yield and the emission efficiency of MPA-capped CdTe quantum dots. The developed approach was employed in the implementation of an automated flow methodology for hydrogen peroxide determination, as this can oxidize GSH preventing its surface passivating effect and producing a manifest fluorescence quenching.

After optimization, linear working calibration curve for hydrogen peroxide concentrations between 0.0025% and 0.040% were obtained ($n=6$), with a correlation coefficient of 0.9975. The detection limit was approximately 0.0012%. The developed approach was employed in the determination of H_2O_2 in contact lens preservation solutions and the obtained results complied with those furnished by the reference method, with relative deviations comprised between −1.18 and 4.81%.

1. Introduction

The surface chemistry of colloidal semiconductor nanocrystals or quantum dots (QDs) is an important parameter determining most of their optical and physical properties, namely their reactivity, luminescence efficiency (quantum yield), photoluminescent properties stability and the solubility in a given solvent [1]. Indeed, the QDs size (usually in the range 1–10 nm) and the resultant quantum confinement effect in combination with the high surface-to-volume ratio and other surface characteristics render QDs photoluminescent properties very sensitive to any micro-environmental change or interaction with a chemical specie [2]. Morphologically, the occurrence of surface imperfections that act as charge carrier traps can impair the efficiency of electron–hole recombination, thus favoring non-radiative recombination processes which can dramatically reduce the fluorescence quantum yield (QY) of QDs [3]. In this regard, surface modification strategies are often used to eliminate trap sites and to increase solution stability preventing aggregation and leading to an enhancement of the QDs luminescent emission intensity [4]. Organic ligands used in the adaption of the surface chemistry provide electronic and chemical passivation of surface traps and enable QDs to be chemically manipulated as large molecules with solubility and reactivity defined by the ligand characteristics [5]. This adaptability has boosted the application of QDs as chemosensors in different analytical applications gaining a wide acceptance among the scientific community. Several works have studied the interaction of quantum dots surface with different substances exhibiting functional groups such as thiol (sulfhydryl) [3,6], amine [7] and phosphonate [4] that could act as enhancers of the fluorescence intensity of QDs. This enhancement was explained by the formation of covalent bonds between the donor atom of the ligand (usually nitrogen, sulfur or oxygen) and incompletely coordinated Cd^{2+} ions on the QDs surface, wherein the referred atoms acted as electron-donors and the dangling orbitals acted as electron-acceptors. Thus, the mid-gap energy states produced by dangling orbitals located between the highest occupied molecular orbital (HOMO) and the lowest unoccupied molecular orbital (LUMO) are effectively removed, thereby preventing the occurrence of non-radiative relaxation pathways.

Glutathione (L-γ-glutamyl-L-cysteinylglycine) is the most abundant intracellular non-protein sulfhydryl compound present in all mammalian tissues participating in numerous cellular functions mainly involving the thiol group of the cysteine residue [8]. In particular, reduced glutathione (GSH) plays an important role in detoxification of hydrogen peroxide, other peroxides, and free radicals [9]. Furthermore, GSH has been widely used as a thiol ligand in the aqueous synthesis of different semiconductor nanocrystals [10,11].

* Corresponding author. Tel.: +351 220428664.
E-mail address: dsmribeiro@gmail.com (D.S.M. Ribeiro).

0039-9140/$ - see front matter © 2014 Elsevier B.V. All rights reserved.
http://dx.doi.org/10.1016/j.talanta.2014.01.031

Hydrogen peroxide is a strong oxidant often used in various industrial and household applications as a bleach or cleaning agent [12]. Owing to its broad antimicrobial activity, H_2O_2 is used for contact lens disinfection, destroying pathogens by triggering oxidative processes. However, depending on the concentration, hydrogen peroxide can be toxic to the ocular epithelium and cornea being necessary to carry out its neutralization before lens wear in order to avoid eyes irritation and possible corneal damage [13]. The wide use of hydrogen peroxide along with the need to assess the efficiency and the safety of its utilization promoted the development of suitable analytical methods for H_2O_2 determination. These include titrimetric [14], electrochemical [15,16], fluorometric [17,18], spectrophotometric [19,20] and chromatographic [21,22] techniques. Additionally, some methodologies based on different flow analysis approaches have been also proposed, including, flow injection analysis with fluorescence [23], chemiluminescence [24], spectrophotometric [25] and amperometric [26] detection. Nevertheless, to the best of our knowledge, the determination of hydrogen peroxide in lens care solutions was only performed by Vidigal et al. [27] wherein a sequential injection lab-on-valve method with spectrophotometric detection was exploited.

In the present work, and for the first time, a novel chemosensor based on GSH-induced fluorescent enhancement of MPA-capped CdTe QDs was developed for hydrogen peroxide determination. With this purpose, the surface interactions between GSH and CdTe nanocrystals were thoroughly evaluated.

The operational characteristics of multipumping flow system (MPFS) [28], namely, low reagents consumption, straightforward automation and control, high portability and versatility allowed to take advantage of particular features of the nanocrystals, such as, the versatile surface chemistry and ligand binding ability for the implementation of a simple, fast and sensitive automatic methodology for the monitoring of hydrogen peroxide in lens care solutions. The analytical methodology was based on the reduction effect of hydrogen peroxide on the GSH-induced fluorescent enhancement of MPA-capped CdTe.

2. Experimental

2.1. Apparatus

The flow manifold comprised of four model 120SP solenoid micropumps (Bio-Chem Valve Inc. Boonton, NJ, USA), which were of the fixed displacement diaphragm type, dispensing 10 μL per stroke. All tubings connecting the different components of the flow system was made of polytetrafluoroethylene PTFE (Omnifit, Cambridge, UK), with 0.8 mm of internal diameter. Homemade end-fittings and acrylic confluence connectors were also used.

The automatic control of the solenoid micro-pumps was accomplished by a microcomputer through the lab-made software developed in Microsoft Visual Basic 6.0®. For the actuation of the micro-pumps a homemade power drive based on the ULN2003 chip was used which was controlled through communication by the computer parallel port.

The detection unit was a spectrofluorometer Jasco (Easton, MD, USA), model FP-2020/2025, equipped with a 16 μL internal volume flow cell.

For the characterization of the synthesized nanoparticles, QDs absorption spectra were obtained by using a Jasco V-660 spectrophotometer (Easton, MD, USA). The fluorescence measurements were performed on a model LS-50B Perkin Elmer luminescence spectrometer (Waltham, MA, USA). A ThermoElectron Jouan BR4I refrigerated centrifuge (Waltham MA, USA) was used for the separation of the precipitated QDs.

FT-IR spectroscopic measurements were carried out using a PerkinElmer Frontier spectrophotometer (Waltham MA, USA) equipped with an universal ATR Diamond/ZnSe support.

The zeta potential of the nanocrystals was obtained using a BI-MAS dynamic light scattering (DLS) instrument (Brookhaven Instruments, USA).

The morphology of the nanoparticles was observed by transmission electron microscopy (TEM) using an electron microscope JEOL JEM 1400 TEM (Tokyo, Japan), at an acceleration voltage of 100 kV, equipped with a Gatan SC 1000 ORIUS CCD camera (Warrendale, PA, USA).

2.2. Samples and standards

All solutions were prepared with water from a Milli-Q system (specific conductivity $\leq 0.1\ \mu S\ cm^{-1}$) and chemicals were of analytical reagent grade quality. Reagents were used as received.

For the assays, a solution containing 1.00 μmol L^{-1} of CdTe QDs was prepared by dissolving 7.84 mg of the synthesized and purified CdTe QDs, with a size of 2.48 nm, in 25 mL of water.

A glutathione solution of 0.651 mmol L^{-1} was daily prepared by dissolving 20 mg of the *L*-glutathione reduced (Sigma, 98% purity, St. Louis MO, USA) in 100 mL of water.

A 0.1% intermediate solution of H_2O_2 was daily prepared by adding, in a 100 mL volumetric flask, 333 μL of hydrogen peroxide (30% w/v, Panreac, Barcelona, Spain) solution and then the volume was made up to the mark with deionized water. The hydrogen peroxide stock solution was standardized by titration with potassium permanganate (Riedel-de Haën, 99% purity, Germany).

The working hydrogen peroxide standard solutions (0.0025–0.040%) were daily prepared by proper dilution of the above intermediate solution by transferring aliquots (1.25–20.0 mL) into a series of 50.00 mL volumetric flasks and the volume was completed to the mark with water.

Five commercially available lens care solutions were analyzed according to the proposed method and no pre-treatment was necessary prior to analysis. Sample solutions were prepared by diluting with deionized water, in 10 mL volumetric flask, an appropriate volume of the lens care solution, in order to obtain a hydrogen peroxide content included in the analytical range of the procedure.

2.3. Reagents and synthesis of CdTe quantum dots

For the synthesis of the CdTe quantum dots, tellurium powder (200 mesh, 99.8%), sodium borohydride ($NaBH_4$, 99%), cadmium chloride hemi(pentahydrate) ($CdCl_2 \cdot 2.5H_2O$, 99%) were purchased from Sigma-Aldrich (St. Louis, MO, USA); 3-mercaptopropionic acid (MPA, 99%) and absolute ethanol (99.5%) were obtained from Fluka (St. Louis MO, USA) and Panreac (Barcelona, Spain) respectively.

Five different diameters of MPA-capped CdTe QDs were synthesized as described by Zou et al. [29] with some modifications. Briefly, the first stage consists on the reduction of tellurium with $NaBH_4$ in N_2 saturated water to produce NaHTe. After all tellurium has been completely consumed the resulting solution was transferred into a second flask containing 4.0×10^{-3} mol of $CdCl_2$ and 6.8×10^{-3} mol of MPA in 100 mL N_2 saturated solution. The pH of the solution was adjusted to 11.5 with a 1.0 mol L^{-1} NaOH solution. The molar ratio of Cd^{2+}:Te^{2-}:MPA was fixed at 1:0.1:1.7. The size of CdTe QDs was controlled by changing the refluxing time.

To purify the CdTe QDs these were precipitated in absolute ethanol to remove the contaminants and the precipitate was subsequently separated by centrifugation, vacuum dried, kept in amber flasks and protected from light.

2.4. Flow manifold

The proposed flow system exploiting the MPFS approach for the fluorometric determination of hydrogen peroxide is depicted in Fig. 1. The flow system was developed with the aim of avoiding the possible interference of H_2O_2 on the fluorescence intensity of QDs allowing, at the same time, a higher sensitivity of the method without impairing the determination rate. For this, GSH was firstly mixed with H_2O_2 creating a first reaction zone which was then mixed with the QDs solution creating a second reaction zone.

Prior to QDs insertion, the simultaneous activation of micro-pumps P_1 and P_2 allowed the combined insertion of GSH and sample solutions through X_1, by exploiting the merging zones approach. The number of pulses was adequate to ensure that the resulting mixed solution filled the reactor coil (RC_1) placed between the confluence points X_1 and X_2 (about 40 cm). Then, the micro-pump P_3 was activated and the QDs solution was inserted into the flow system reaching the confluence point X_2. Finally, through the actuation of the micro-pump P_4, the exceeding volumes of the reagents solutions were rejected to waste and the baseline was established with H_2O. Thus, all flow tubings were filled with the corresponding solution.

The analytical cycle started with the insertion of a pre-set number of plugs of QDs solution intercalated with plugs of the pre-mixed sample/GSH solution. This sampling stage consisted in the insertion of one pulse of QDs solution between two pulses of the pre-mixed sample/GSH solution through the alternated activation of the micro-pumps P_1, P_3 and P_2, by this order, at a fixed pulse time of 0.2 s. This procedure was repeated for a pre-selected number of aliquots thus defining the volumes of the pre-mixed sample/GSH and QDs solutions inserted in the flow system. Subsequently, the reaction zone was carried towards the detector through the repeated actuation of P_4 (10 μL per stroke), at a fixed pulse time of 0.6 s, corresponding to a pulse frequency of 80 min^{-1}, which defined the flow rate at 0.80 mL min^{-1}. The fluorescence emission was monitored at 546 nm (λ_{ex}=400 nm).

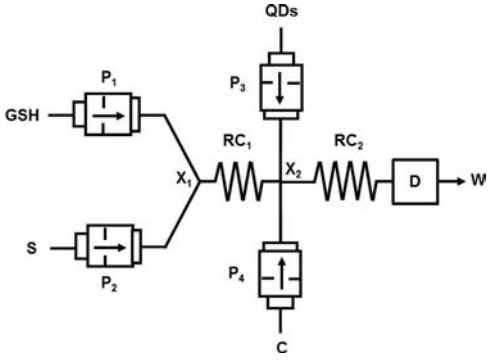

Fig. 1. Multipumping flow manifold. P_1–P_4: solenoid micro-pumps (10 μL stroke volumes); X_1 and X_2, confluence points; RC_1: 40 cm reactor coil; RC_2: 75 cm reactor coil; D, fluorescence detector; GSH, glutathione prepared in deionized water; S, sample (H_2O_2); QDs, MPA-CdTe quantum dots prepared in deionized water; C, carrier solution (deionized water); and W, waste.

3. Results and discussion

3.1. Characterization of quantum dots

The optical properties of the as-prepared MPA-capped CdTe QDs were characterized by absorption and fluorescence spectroscopy (Fig. 2(A) and (B)). All nanocrystals exhibited a well-defined absorption maximum for the first excitonic transition and a narrow and symmetric fluorescence spectra with FWHM (Full Width at Half Maximum) values in the range from 43 to 55 nm, evidencing that the CdTe QDs were nearly monodisperse and homogeneous.

The sizes of the synthesized QDs were calculated by the following equation [30]:

$$D=(9.8127\times10^{-7})\lambda^3-(1.7147\times10^{-3})\lambda^2+(1.0064)\lambda-(194.84)$$

where D is the diameter (nm) and λ (nm) the wavelength of

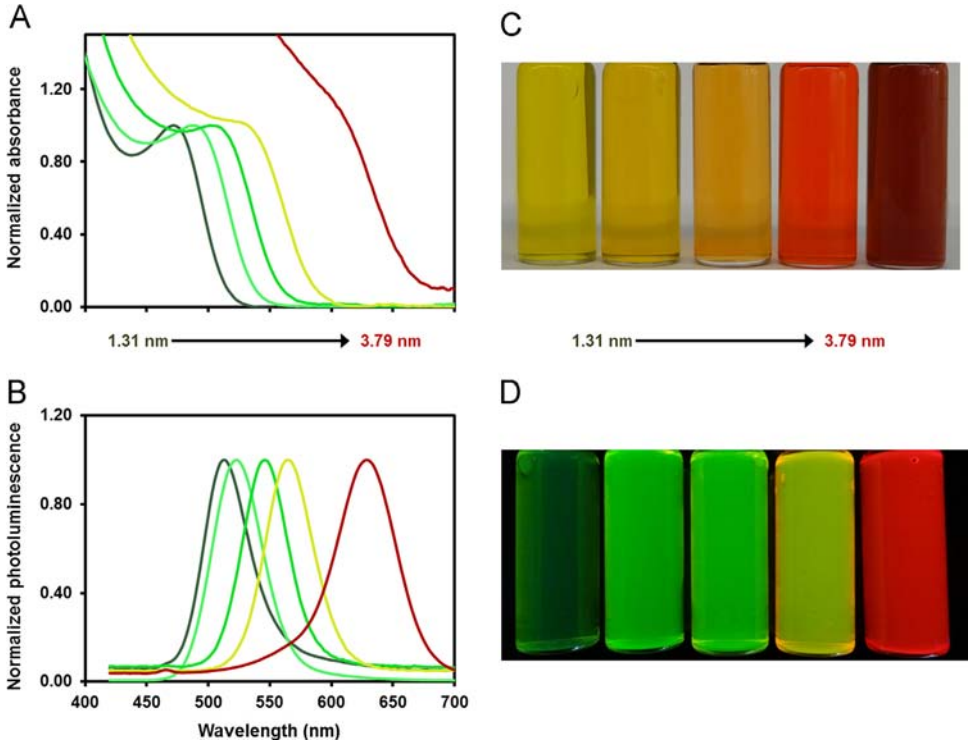

Fig. 2. Normalized absorption (A) and photoluminescence (B) spectra of the different sizes of QDs. Photograph of the QDs solutions without irradiation (C) and irradiated with UV light at 365 nm (D).

maximum absorbance corresponding to the first excitonic absorption peak of the nanocrystal. Thus, five different nanoparticles sizes, namely 1.36, 1.98, 2.48, 3.01 and 3.79 nm, were synthesized, which maximum absorption wavelengths were observed at 472, 488, 505, 532 and 614 nm, respectively.

The morphology of 2.48 nm CdTe QDs was investigated by transmission electron microscopy (TEM). Fig. 3 showed that the nanoparticles, with an average size around the diameter calculated by Yu et al. [30], are monodispersed and their shape is close to spherical.

The molar concentration of the different sized nanocrystals in solution was determined by establishing firstly the extinction coefficient (ε) using the expression:

$\varepsilon = 3450\Delta E(D)^{2.4}$ where ΔE is the transition energy corresponding to the first absorption peak expressed in eV. By knowing ε and the absorbance of a known concentration solution, the molar concentration was estimated by applying the Lambert–Beer's law.

3.2. Preliminary assays

Preliminary batch assays involving steady-state fluorescence spectroscopy measurements were conducted in order to evaluate the interaction between MPA-CdTe QDs and glutathione. For each of the synthesized nanoparticles with sizes of 1.36, 1.98, 2.48, 3.01 and 3.79 nm several solutions were prepared containing 3.0 μmol L^{-1} of MPA-CdTe QDs and increasing concentrations of glutathione in a range of 0–9.76 mmol L^{-1}. The emission spectra of all solutions were recorded upon excitation at 400 nm. The obtained results showed (Fig. 4(A)) that for all synthesized sizes the QDs fluorescence gradually increased with increasing GSH concentration. Additionally, with the increase of QDs size it was necessary to add ever-increasing concentrations of glutathione to reach the maximum fluorescence enhancement, as shown in Table 1. However, it was observed that after reaching the highest fluorescence enhancing subsequent GSH concentration increments led to a precipitation of the nanoparticles that caused a corresponding fluorescence reduction and a red shift of the maximum wavelength emission. This phenomenon can be related to the alteration of the electric charge on QDs surface which induced the aggregation of the nanoparticles and the consequent energy transfer between QDs aggregates. In order to ascertain this theory, the zeta potential of two different solutions, containing (i) 3.0 μmol L^{-1} CdTe QDs (2.48 nm) and (ii) a mixture of 3.0 μmol L^{-1} of the QDs (2.48 nm) and 1.63 mmol L^{-1} of glutathione was measured. Aiming to eliminate the excess of glutathione, the second solution was precipitated with ethanol, centrifuged and re-dissolved with deionized water. The zeta potential of the QDs solution was -47.83 ± 1.65 mV and that of the mixture of QDs and glutathione was -33.85 ± 0.84 mV. The decrease of the absolute value of zeta potential demonstrate alterations on the surface charge of QDs, which justified their instability in solution and the increased tendency to aggregate.

The preliminary assays also revealed that the maximum fluorescence intensity enhancement was obtained for QDs with sizes of 1.36 and 2.48 nm. For the biggest QDs (3.79 nm) the fluorescence enhancement was not as evident as for the remaining QDs which might be due to self-quenching or re-absorption phenomena.

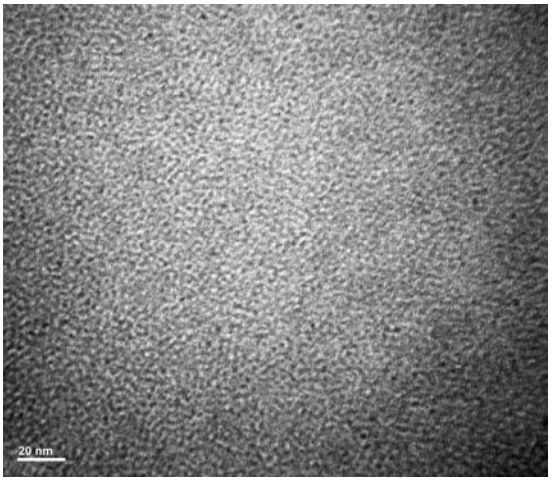

Fig. 3. TEM images of the 2.48 nm MPA-CdTe QDs.

3.3. Mechanism investigation of the interaction between MPA-CdTe QDs and glutathione

The possible interaction mechanism of glutathione and CdTe QDs was also investigated aiming to understand what happens at

Table 1
Compilation of the obtained results of the enhancing effect of glutathione concentration on the fluorescence intensity of the different MPA-CdTe QDs sizes.

MPA-CdTe QDs Size	$[GSH]_{added}$ (mmol L^{-1})	Maximum FI enhancement (%)	Red-shift of maximum wavelength emission (nm)
1.36 nm	0.33	384.65	513–517
1.98 nm	0.98	304.60	530–540
2.48 nm	1.63	336.01	546–551
3.01 nm	1.95	248.45	565–571
3.79 nm	6.51	48.18	n/a

n/a–not applicable.

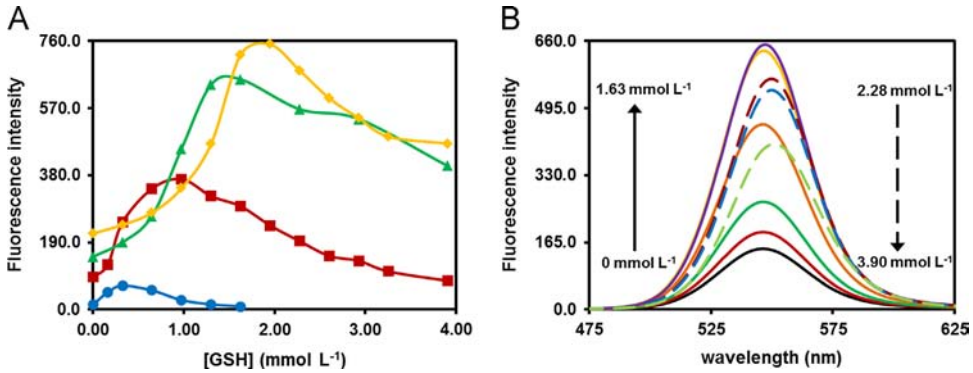

Fig. 4. (A) Influence of different GSH concentrations on the fluorescence intensity of 3.0 μmol L^{-1} MPA-CdTe QDs with different sizes: (●) 1.36 nm; (■) 1.98 nm; (▲) 2.48 nm; (◆) 3.01 nm. (B) Fluorescence emission spectra of 3.0 μmol L^{-1} MPA-CdTe with a size of 2.48 nm in the presence of different GSH concentrations: (——) 0 mmol L^{-1}; (——) 0.33 mmol L^{-1}; (——) 0.65 mmol L^{-1}; (——) 0,98 mmol L^{-1}; (——) 1.30 mmol L^{-1}; (——) 1.63 mmol L^{-1}; (— —) 2.28 mmol L^{-1}; (— —) 2.93 mmol L^{-1}; and (— —) 3.90 mmol L^{-1}.

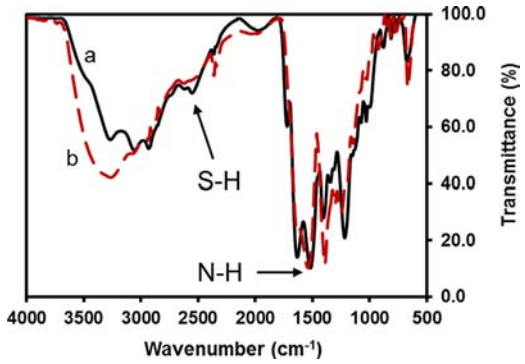

Fig. 5. FT-IR spectra of (a) glutathione (—) and (b) the interaction of glutathione with MPA-CdTe QDs (— —).

the surface of the nanoparticles that leads to the enhancement of fluorescence emission. Considering that glutathione contains several functional groups, such as thiol, amine and carboxylic acid, which can interact with the QDs surface, FT-IR measurements were performed in order to identify whether some of these groups are responsible for the binding of glutathione to MPA-CdTe. For the FT-IR measurements, two different solutions were prepared (1.63 mmol L^{-1} of glutathione in deionized water and 3.0 μmol L^{-1} of 2.48 nm MPA-CdTe QDs with 1.63 mmol L^{-1} of glutathione in deionized water), and the corresponding FT-IR spectra were compared (Fig. 5). Both solutions were previously lyophilized with the aim of circumvent the interference of water in the FT-IR spectra.

The obtained results showed that upon interaction of GSH with MPA-CdTe QDs the typical GSH thiol (S–H) stretching vibrational band (2550–2678 cm^{-1}) disappeared. For this reason it can be assumed that the most probable reaction mechanism is the complexation of incompletely bounded cadmium ions on the QDs surface by GSH thiol group, as already mentioned in previous works [3,6]. The surface defects sites are crystal imperfections due to the presence of atoms with dangling bonds. These defects produce energy states within the quantum dots bandgap facilitating the non-radiative recombination which lead to weaker quantum yield of the QDs nanoparticles [31]. The thiol group of GSH molecules bind to these surface defects sites effectively removing the traps states which improve QDs passivation and consequently increasing the intensity of photoluminescence emission.

The involvement of other functional groups of GSH on the interaction with the MPA-CdTe cannot be completely excluded because both the carboxylic acid and the amines are susceptible to coordinate cadmium ions on the surface of the quantum dots. However, taking into account the scientific literature information that refers the higher affinity of thiol group for binding heavy metals [32,33] and also the obtained FT-IR spectra displayed in Fig. 5, the most probable interaction mechanism involves the binding of the GSH thiol group to the surface of QDs through the formation of Cd–S covalent bonds.

3.4. Optimization of the MPFS

Aiming to develop a simple, fast and automatic QDs-based analytical methodology for the determination of hydrogen peroxide, the study of the surface interactions between glutathione and MPA-CdTe nanocrystals was implemented in a miniaturized and automatic analytical flow system based in the multipumping concept. Thus, an optimization assay, in order to evaluate the fluorescence enhancing effect (ΔFE (%)) of the interaction of several GSH concentrations with five different sized QDs and, at same time, different QDs concentrations, was performed using an initial manifold (Fig. 1 in Supplementary material). This MPFS manifold consisted in three micro-pumps, a 50 cm reactor coil and a fluorescence detector, in which, two micro-pumps were responsible for the QDs and GSH insertion and the last one was used to propel the carrier solution (deionized water).

In this assay, it was evaluated the fluorescence enhancing of QDs upon reaction with GSH at concentrations ranging from 0 to 19.52 mmol L^{-1}. Since the size of the nanoparticles is well-known to have a strong effect on the physical properties of the QDs defining its reactivity and the magnitude of the analytical signal, the influence of GSH on different QDs sizes and concentrations, were assayed. Nanoparticles of 1.36, 1.48 and 2.48 nm were used in concentrations of 1.0, 3.0 and 5.0 μmol L^{-1} and the QDs of sizes 3.01 and 3.79 nm were tested in the concentrations of 0.25, 0.50, 1.0, 3.0 and 5.0 μmol L^{-1}.

The obtained results in this assay, depicted in Fig. 6, seem to support the conclusions drawn from preliminary assays.

In fact, for each size of QDs tested it was observed that by increasing the concentration of GSH, the analytical signal increased up to a certain value from which a decrease was noted due to the reasons already explained in Section 3.2 (Preliminary assays). The GSH concentration that needs to be added to achieve the maximum fluorescence enhancing effect (ΔFE (%)) depended on the size and concentration of the QDs. Thus, for higher sizes and concentrations of QDs it was verified that an increased GSH concentration was required to obtain the maximum fluorescence enhancing effect, as it can be seen on Table 2. Additionally, it was noticed that for QDs with sizes of 1.36, 1.98, 2.48 nm the analytical signal (fluorescence enhancing effect) increased up to 3 μmol L^{-1} and then decreased, while for the bigger QDs sizes (3.01 and 3.79 nm) ΔFE (%) increased up to 1 μmol L^{-1} diminishing for higher QDs concentrations values. This fact can be related to the inner filter effect because when the QDs concentration reaches high values self-quenching or re-absorption of emitted radiation can occur leading to a decrease of fluorescence. The inner filter effect can also explain the fact that the initial fluorescence of 3.79 nm QDs was unexpectedly low and that upon GSH addition the fluorescence enhancing effect was not as evident as with the other tested QDs sizes.

The results also revealed that the highest fluorescence enhancing effect was obtained for 1.36 nm QDs at concentration of 3.0 μmol L^{-1} and for 2.48 nm QDs at concentrations of 1.0 and 3.0 μmol L^{-1}. For QDs with 2.48 nm the analytical signal obtained (ΔFE (%)) was similar for concentration of 1.0 and 3.0 μmol L^{-1}, however the GSH concentration needed to obtain the maximum fluorescence enhancing effect increased from 0.813 to 3.90 mmol L^{-1}. Thus, considering the previous results and aiming to obtain a better agreement between reagents consumption, sensitivity and detection limit, the following optimization assays were performed only for QDs with sizes of 1.36 and 2.48 nm at concentrations of 3.0 and 1.0 μmol L^{-1}, respectively.

The higher reactivity exhibited by QDs with sizes of 1.36 and 2.48 nm can be justified by the presence of a greater number of surface defects that can coordinate with the GSH thiol group.

For the purpose of applying this methodology to the determination of hydrogen peroxide in lens care solutions, the configuration of the initial multipumping flow manifold was modified as depicted in Fig. 1. Upon the modification of the flow system and with the aim of obtaining the optimal chemical conditions with respect to the size and concentration of QDs and also the GSH concentration, the study of the surface interactions between glutathione and MPA-CdTe QDs was repeated for 1.36 and 2.48 nm QDs at concentrations of 3.0 and 1.0 μmol L^{-1}, respectively. For QDs sizes of 2.48 nm at 1.0 μmol L^{-1} a maximum fluorescence enhancing effect of 389% was obtained upon GSH addition of 0.651 mmol L^{-1} while for the smaller QDs (1.36 nm) at 3.0 μmol L^{-1} the higher value of ΔFE was 291% when a GSH

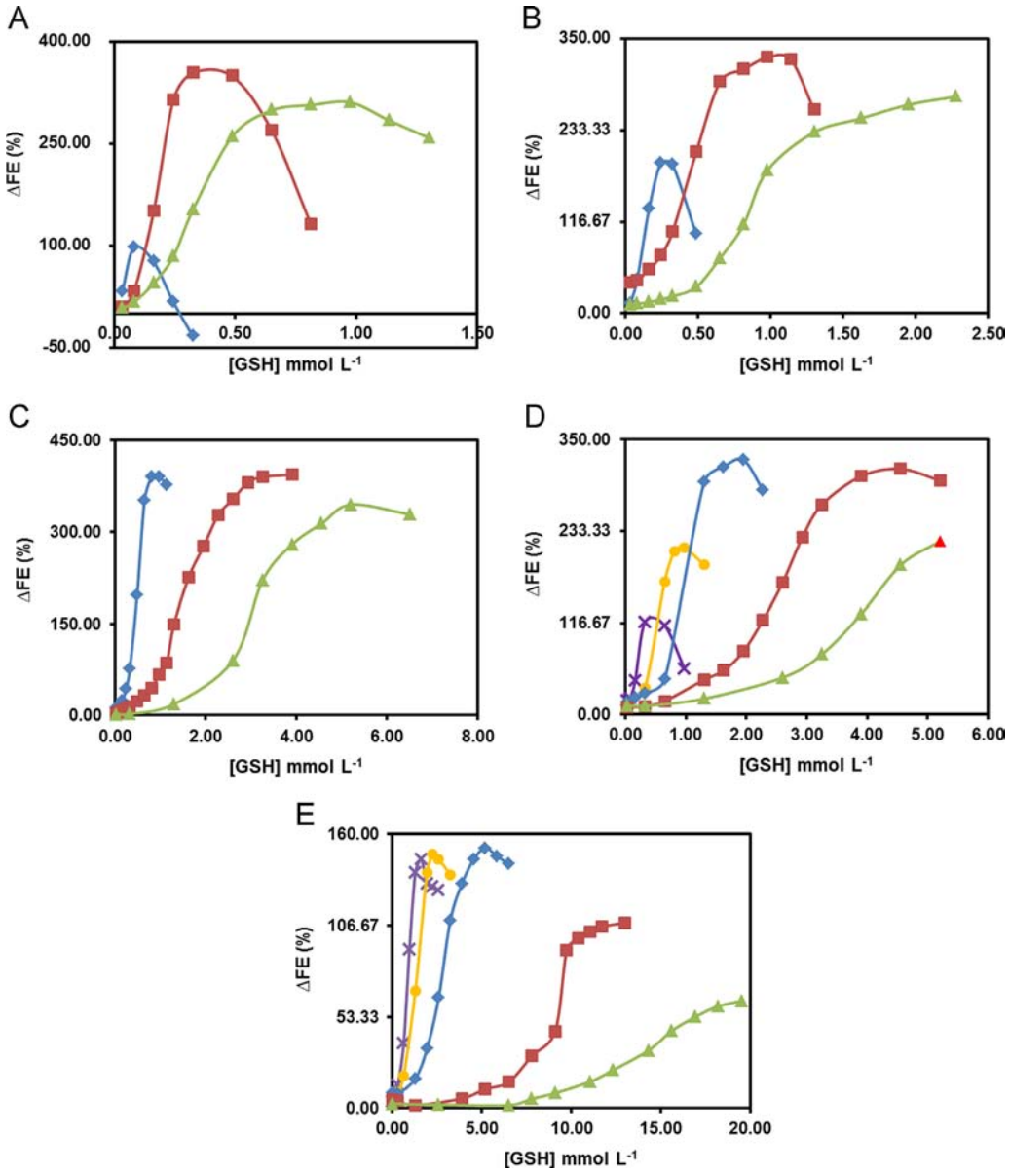

Fig. 6. Evaluation of the fluorescence enhancing effect upon the interaction of different GSH concentrations to MPA-CdTe QDs with different sizes; (a) 1.36 nm; (b) 1.98 nm; (c) 2.48 nm; (d) 3.01 nm; (e) 3.79 nm and different QDs concentrations; (×) 0.25 μmol L^{-1}; (●) 0.50 μmol L^{-1}; (◆) 1.0 μmol L^{-1}; (■) 3.0 μmol L^{-1}; and (▲) 5.0 μmol L^{-1}.

Table 2
Results obtained in study of the influence on the fluorescence enhancing effect upon the interaction of different GSH concentrations to QDs with different sizes and concentrations.

QDs size (nm)	[MPA-CdTe QD]									
	0.25 μmol L^{-1}		0.5 μmol L^{-1}		1.0 μmol L^{-1}		3.0 μmol L^{-1}		5.0 μmol L^{-1}	
	$[GSH]_{added}$ (mmol L^{-1})	ΔFE (%)	$[GSH]_{added}$ (mmol L^{-1})	ΔFE (%)	$[GSH]_{added}$ (mmol L^{-1})	ΔFE (%)	$[GSH]_{added}$ (mmol L^{-1})	ΔFE (%)	$[GSH]_{added}$ (mmol L^{-1})	ΔFE (%)
1.36	–	–	–	–	0.081	97.42	0.33	354.37	0.98	310.94
1.98	–	–	–	–	0.244	191.61	0.98	326.04	2.28	276.35
2.48	–	–	–	–	0.813	390.33	3.90	393.50	3.90	175.70
3.01	0.33	117.84	0.98	211.74	1.952	323.98	4.56	312.54	5.21	220.52
3.79	1.63	145.04	2.28	148.09	5.206	151.88	13.02	108.23	19.52	62.61

concentration of 0.325 mmol L^{-1} was added. An evaluation of the obtained results showed that an analytical signal (ΔFE (%)) improvement of about 34% was observed for QDs size of 2.48 nm at 1.0 μmol L^{-1} regarding the 1.36 nm QDs at 3.0 μmol L^{-1}. Accordingly, considering the final application of the developed methodology the 2.48 nm QDs at a concentration of 1.00 μmol L^{-1} and a GSH concentration of 0.651 mmol L^{-1} were selected for subsequent assays.

The succeeding experiments were carry out with the purpose of evaluating the influence on the analytical signal of the physical flow parameters such as reactor length, sample and reagent volumes and flow rate aiming to achieve the better compromise between sensitivity, reagent consumption and determination rate.

The study of the influence of the reactor length on the sensitivity of the methodology was performed simultaneously with the inserted sample/reagents volumes. In these assays, for every reactor's length evaluated, namely 25, 50, 75 and 100 cm, the number of sample/reagents pulses was varied between 4 and 12 (corresponding to volumes between 40 and 120 μL). In addition, for all lengths and number of pulses assayed, calibration curves were established for hydrogen peroxide concentrations between 0.0025 and 0.040% (w/v) in order to evaluate the sensitivity of the methodology through the analysis of the obtained slopes. This study allowed concluding that the reactor's length was the parameter with the most pronounced influence on the sensitivity of the methodology, showing an accentuated increase on the sensitivity up to 75 cm and subsequent stabilization for higher values (Fig. 7, graphic A). In opposition, sample and reagents volumes had a minor influence on sensitivity. By using a 75 cm reactor and increased number of sample pulses an increment of the sensitivity was observed for up to 8 pulses followed by a decrease for higher values (Fig. 7, graphic B). Consequently, for the posterior assays a reactor length of 75 cm and 8 pulses of sample and reagents (corresponding to a volume of 80 μL) were chosen.

Another flow parameter that could have a noteworthy effect on the methodology sensitivity was flow rate as it determines the residence time of the reaction zone within the flow system and hence the reaction time. In these assays, for different pulse times of 0.15, 0.30, 0.45, 0.60 and 0.75 s (corresponding to flow rates of 2.00, 1.33, 1.00, 0.80, 0.67 mL min^{-1}), calibration curves for hydrogen peroxide concentrations ranging from 0.0025 to 0.040% (w/v), were obtained.

The obtained results (Fig. 8) revealed that the sensitivity of the methodology slightly increased by varying the flow rate between 0.67 and 0.80 mL min^{-1} while for higher values markedly decreased. For this reason, the latter flow rate (corresponding to a pulse time of 0.60 s) was selected for the assays.

Taking into consideration the results obtained in the physical optimization it was possible to conclude that the reaction kinetics was low because the combination of a long reactor (75 cm) and a low flow rate (0.80 mL min^{-1}) determine a considerable residence time of the reaction zone inside the flow system that could give rise to a major sample dispersion. In this particular, the pulsed flow produced by the solenoid micro-pumps acts favorably regarding conventional laminar flow regimens.

3.5. Mechanism of the hydrogen peroxide determination

The hydrogen peroxide determination was based on the monitoring of the reduction of the fluorescence enhancing effect of MPA-CdTe QDs upon interaction with glutathione in aqueous solution. As above referred, the GSH was used to improve the surface passivation of the MPA-capped CdTe QDs thus providing a fluorescent probe with enhanced fluorescence. Therefore, in the absence of hydrogen peroxide, the obtained signal was maximum (blank signal) since all GSH was available for the surface passivation of QDs. In the presence of hydrogen peroxide, most of the glutathione (GSH) was oxidized to glutathione disulfide (GSSG) and the number of SH group available for the establishment of the Cd–S covalent bonds between GSH and the QDs surface markedly decreased. Thus, the higher the hydrogen peroxide concentration the more pronounced the reduction of free GSH. Consequently, the surface passivation of the QDs is attenuated, traps states removal is

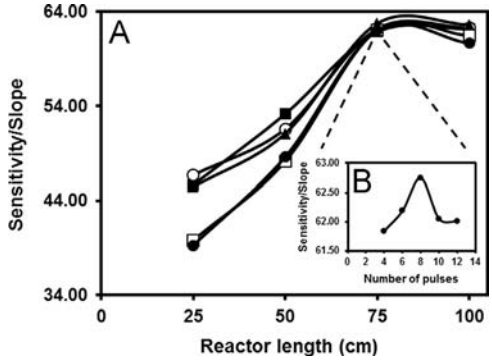

Fig. 7. Influence of the reactor length and number of sample pulses (sample volume) on the sensitivity of the methodology. (■) 4 pulses; (◯) 6 pulses; (▲) 8 pulses; (□) 10 pulses; and (●) 12 pulses.

Table 3
Comparison of the analytical results obtained in the determination of hydrogen peroxide in commercial lens care solutions by the proposed flow procedure and the reference procedure.

Sample	Declared amount (%)	Amount found (%)		R.D %[b]
		MPFS methodology[a]	Reference method	
Oxysept®	3	2.92 ± 0.04	2.87 ± 0.01	1.56
iWear®	3	3.31 ± 0.04	3.34 ± 0.02	−1.18
D'Afflelou®	3	2.79 ± 0.07	2.81 ± 0.01	−0.75
Disco®	3	3.28 ± 0.04	3.13 ± 0.03	4.81
AO sept®	3	3.5 ± 0.1	3.51 ± 0.02	0.72

[a] Mean ± $t0.05$ (Student's t test) × ($s/\sqrt{n}$).
[b] Relative deviation of the developed method regarding the reference procedure.

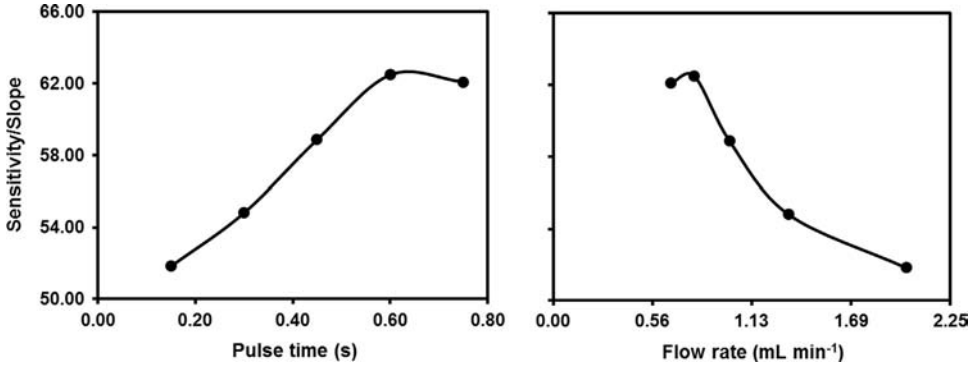

Fig. 8. Influence of the micro-pumps pulse time and the corresponding flow rate on the sensitivity of the methodology.

impaired and the fluorescence enhancing effect is restrained (quenching of analytical signal). The observed inhibition of the fluorescence enhancing effect (when compared to the blank reading) was used to quantify the hydrogen peroxide amount in lens care solutions.

3.6. Figures of merit of the method

After establishing the chemical and physical conditions of the flow system, it was possible to achieve a linear relationship between the magnitude of analytical signal and the logarithmic of H_2O_2 concentration in the range of 0.0025–0.040%. Thus, the analytical curve was typically described by the equation:

$$\Delta FE = -64(\pm 2) \times \text{Log } C + 186(\pm 4) (R = 0.9975,\ n = 6)$$

where ΔFE was the analytical signal, expressed in percentage and C was the hydrogen peroxide concentration. The detection limit calculated from the equation of the calibration curve [34] was about 0.0012%. The developed methodology allowed a determination rate of about 54 h^{-1}, corresponding to the analysis of about 14 samples per hour (considering the time required for sample replacement).

3.7. Method validation

In order to validate the reliability of the proposed automatic methodology, the hydrogen peroxide monitoring in five commercially available lens care solutions was performed by the developed MPFS and the obtained results were compared with those furnished by the reference procedure [35]. The reference methodology recommended by the European Pharmacopoeia [35] involved a titration of the hydrogen peroxide with potassium permanganate in acidic medium. The hydrogen peroxide amount in the tested samples was evaluated considering that each mL of 0.02 mol L^{-1} $KMnO_4$ solution was equivalent to 1.701 mg of H_2O_2. The results are shown in Table 3 and indicated a good agreement between both methods with relative deviations between −1.18 and 4.81%. Moreover, the obtained results were statistically compared for accuracy and precision. The paired Student's t-test and variance F-test [34] confirmed that there were no significant differences between the results obtained by both procedures ($t_{calculated} = 0.960$, $t_{tabulated} = 2.776$ and $F_{calculated} = 1.034$, $F_{tabulated} = 6.388$; $n = 5$) with respect to accuracy and precision, for a confidence level of 95%.

The precision of the proposed methodology was evaluated through the repeated analysis of each sample solution (three determinations for each sample), which revealed a good repeatability taking into account the calculated concentration ranges for a confidence level of 95%.

Concerning the selectivity of the proposed methodology, it was observed no influence on the analytical signal caused by the presence of the chemical species commonly used in the composition of the lens care solutions since pronounced sample dilutions were performed before the analysis.

4. Conclusions

This work demonstrated that reduced glutathione can effectively enhance the fluorescence properties of MPA-capped CdTe QDs as a result of the passivation of the nanocrystals surface trap states through the binding of GSH thiol group to Cd^{2+}. Additionally, it was observed that the fluorescence enhancing effect is markedly affected by the size and concentration of the nanoparticles and also by the GSH concentration added. Indeed, depending on the size and concentration of the nanoparticles and for GSH concentrations excessively high it was verified a decrease of QDs solution stability as they tended to aggregate and precipitate resulting in a fluorescence decrease.

For the first time, a novel sensitive detecting technique based on GSH-induced fluorescent enhancement of MPA-capped CdTe QDs was developed and successfully used for the determination of hydrogen peroxide in lens care solutions. The fluorometric determination of hydrogen peroxide was efficaciously implemented in an automatic multi-pumping flow system which allowed a strict and reproducible control of the QDs/GSH/H_2O_2 reaction conditions and high versatility in terms of solutions manipulation. In addition, the multi-pumping approach demonstrated to be a potential tool for automation of QDs-based sensing schemes involving surface ligand interactions since accurate, precise and reliable results were obtained assuring, at same time, high sample throughput and low reagents consumption.

Acknowledgments

S. Sofia M. Rodrigues thanks the “Fundação para a Ciência e Tecnologia” and FSE (Quadro Comunitário de Apoio) for the Ph.D. Grant (SFRH/BD/70444/2010). Authors are also grateful to FCT for the financial support under Project (PTDC/QUI-QUI/105514/2008) under COMPETE/QREN/FEDER.

Appendix. Supplementary materials

Supplementary data associated with this article can be found in the online version at http://dx.doi.org/10.1016/j.talanta.2014.01.031.

References

[1] Z. Yuan, P. Yang, Mater. Res. Bull. 48 (2013) 2640–2647.
[2] C. Frigerio, D.S.M. Ribeiro, S.S.M. Rodrigues, V.L.R.G. Abreu, J.A.C. Barbosa, J.A.V. Prior, K.L. Marques, J.L.M. Santos, Anal. Chim. Acta 735 (2012) 9–22.
[3] Y.-S. Xia, C.-Q. Zhu, Microchim. Acta 164 (2009) 29–34.
[4] Z. Liu, S. Liu, P. Yin, Y. He, Anal. Chim. Acta 745 (2012) 78–84.
[5] V.I. Klimov, Semiconductor and Metal Nanocrystals: Synthesis and Electronic and Optical Properties, Marcel Dekker Incorporated, New York, 2003.
[6] C. Frigerio, V.L.R.G. Abreu, J.L.M. Santos, Talanta 96 (2012) 55–61.
[7] G.-L. Wang, H.-J. Jiao, X.-Y. Zhu, Y.-M. Dong, Z.-J. Li, Talanta 93 (2012) 398–403.
[8] A. Meister, M.E. Anderson, Annu. Rev. Biochem. 52 (1983) 711–760.
[9] A. Pastore, F. Piemonte, M. Locatelli, A. Lo Russo, L.M. Gaeta, G. Tozzi, G. Federici, Clin. Chem. 47 (2001) 1467–1469.
[10] Y.-H. Zhang, H.-S. Zhang, M. Ma, X.-F. Guo, H. Wang, App. Surf. Sci. 255 (2009) 4747–4753.
[11] J.L. Gautier, J.P. Monrás, I.O. Osorio-Román, C.C. Vásquez, D. Bravo, T. Herranz, J.F. Marco, J.M. Pérez-Donoso, Mater. Chem. Phys. 140 (2013) 113–118.
[12] I.L.d. Mattos, K.A. Shiraishi, A.D. Braz, J.R. Fernandes, Quím. Nova 26 (2003) 373–380.
[13] R. Hughes, S. Kilvington, Antimicrob. Agents Chemother. 45 (2001) 2038–2043.
[14] A. Brestovisky, E. Kirowaeisner, J. Osteryoung, Anal. Chem. 55 (1983) 2063–2066.
[15] K.-C. Lin, C.-Y. Yin, S.-M. Chen, Sens. Actuator B–Chem. 157 (2011) 202–210.
[16] K. De Wael, Q. Bashir, S. Van Vlierberghe, P. Dubruel, H.A. Heering, A. Adriaens, Bioelectrochemistry 83 (2012) 15–18.
[17] H. Chen, H. Yu, Y. Zhou, L. Wang, Spectrochim. Acta A 67 (2007) 683–686.
[18] M.E. Abbas, W. Luo, L. Zhu, J. Zou, H. Tang, Food Chem. 120 (2010) 327–331.
[19] S.B. Mathew, A.K. Pillai, V.K. Gupta, J. Dispers. Sci. Technol. 30 (2009) 609–612.
[20] K. Sunil, B. Narayana, Bull. Environ. Contam. Toxicol. 81 (2008) 422–426.
[21] J. Liu, S.M. Steinberg, B.J. Johnson, Chemosphere 52 (2003) 815–823.
[22] S. Steinberg, Environ. Monit. Assess. 185 (2013) 3749–3757.
[23] S. Svensson, A.-C. Olin, M. Lärstad, G. Ljungkvist, K. Torén, J. Chromatogr. B 809 (2004) 199–203.
[24] H. Chen, L. Lin, Z. Lin, C. Lu, G. Guo, J.-M. Lin, Analyst 136 (2011) 1957–1964.
[25] M. Kurihara, M. Muramatsu, M. Yamada, N. Kitamura, Talanta 96 (2012) 180–184.
[26] R.C. Matos, J.J. Pedrotti, L. Angnes, Anal. Chim. Acta 441 (2001) 73–79.
[27] S.S.M.P. Vidigal, I.V. Tóth, A.O.S.S. Rangel, Microchem. J. 91 (2009) 197–201.
[28] R.A.S. Lapa, J.L.F.C. Lima, B.F. Reis, J.L.M. Santos, E.A.G. Zagatto, Anal. Chim. Acta 466 (2002) 125–132.

[29] L. Zou, Z. Gu, N. Zhang, Y. Zhang, Z. Fang, W. Zhu, X. Zhong, J. Mater. Chem. 18 (2008) 2807–2815.
[30] W.W. Yu, L.H. Qu, W.Z. Guo, X.G. Peng, Chem. Mater. 15 (2003) 2854–2860.
[31] U. Woggon, Optical Properties of Semiconductor Quantum Dots, Springer-Verlag GmbH, Germany, 1997.
[32] D. Kolb, M. Mueller, G. Zellnig, B. Zechmann, Protoplasma 243 (2010) 87–94.
[33] M. Jozefczak, T. Remans, J. Vangronsveld, A. Cuypers, Int. J. Mol. Sci. 13 (2012) 3145–3175.
[34] J.N. Miller, J.C. Miller, Statistics and Chemometrics for Analytical Chemistry, 6th ed., Prentice Hall/Pearson, England, 2010.
[35] Council of Europe, European Pharmacopoeia, 5th ed., , 2004.